

M-CALLM: Multi-level Context Aware LLM Framework for Group Interaction Prediction

Diana Romero

dgromer1@uci.edu

University of California, Irvine

Daniel Khalkhali

dkhalkha@uci.edu

University of California, Irvine

Xin Gao

xgao10@uci.edu

University of California, Irvine

Salma Elmalaki

salma.elmalaki@uci.edu

University of California, Irvine

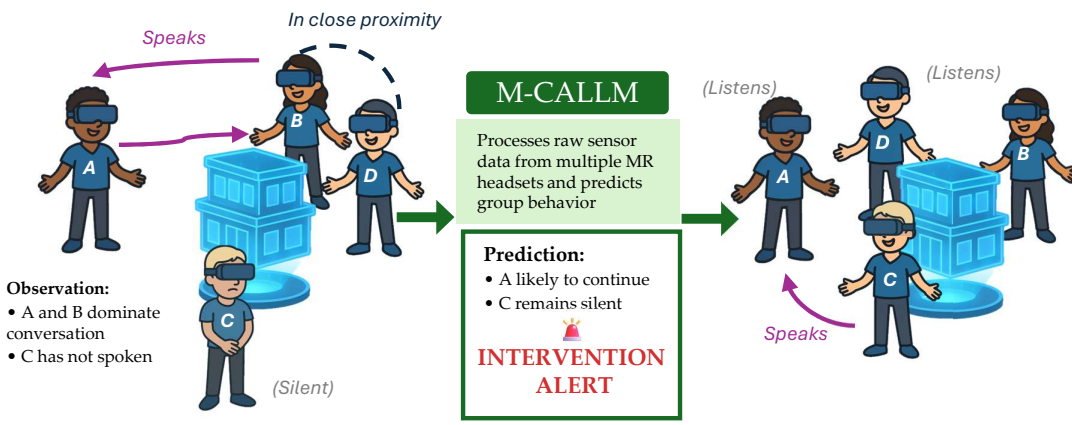


Figure 1: Real-time coordination support in collaborative MR environments. M-CALLM observes current group behavior (centralized conversation with participants A and B dominating while C remains silent), encodes multi-level context, predicts future interaction patterns, and generates timely intervention alerts to prevent communication bottlenecks before they occur. The avatars are generated by DALL-E [39].

Abstract

This paper explores how large language models can leverage multi-level contextual information to predict group coordination patterns in collaborative mixed reality environments. We demonstrate that encoding individual behavioral profiles, group structural properties, and temporal dynamics as natural language enables LLMs to break through the performance ceiling of statistical models. We build **M-CALLM**, a framework that transforms multimodal sensor streams into hierarchical context for LLM-based prediction, and evaluate three paradigms (zero-shot prompting, few-shot learning, and supervised fine-tuning) against statistical baselines across intervention mode (real-time prediction) and simulation mode (autoregressive forecasting). Head-to-head comparison on 16 groups (64 participants, ~25 hours) demonstrates that context-aware LLMs achieve 96% accuracy for conversation prediction, a 3.2 \times improvement over LSTM baselines, while maintaining sub-35ms latency. However, simulation mode reveals brittleness with 83% degradation due to cascading errors. Deep-dive into modality-specific performance shows conversation depends on temporal patterns, proximity benefits from group structure (+6%), while shared attention fails completely (0% recall), exposing architectural limitations. We hope this work spawns new ideas for building intelligent collaborative sensing systems that balance semantic reasoning capabilities with fundamental constraints.

CCS Concepts

- Computing methodologies → Machine learning; Modeling and simulation;
- Human-centered computing → Collaborative and social computing; Mixed / augmented reality.

Keywords

Context-aware LLMs, Group behavior prediction, Multimodal sensing

1 Introduction

Collaborative Mixed Reality (MR) environments are transforming how people work together, enabling remote teams to manipulate shared virtual objects, coordinate spatial tasks, and communicate through embodied interaction [5, 42]. Unlike traditional video conferencing, MR collaboration generates rich multimodal behavioral data including gaze patterns revealing attention focus, proximity metrics capturing spatial coordination, and conversation dynamics showing information exchange. This wealth of sensor data presents an opportunity: can we predict *how* groups will interact in the near future, enabling systems to provide timely interventions, simulate team behaviors, or optimize collaborative workflows?

Accurately sensing and predicting group behavior is critical for team effectiveness because it enables proactive coordination support (Figure 1): systems can detect emerging communication bottlenecks (e.g., one member dominating discussion), anticipate attention fragmentation before it occurs, and recommend interventions at moments when the group is most receptive to change [37, 51]. Beyond real-time interventions, behavioral prediction supports team composition optimization by identifying collaboration patterns that correlate with task success, enables virtual agents to adapt their participation based on forecasted group states, and allows facilitators to simulate “what-if” scenarios for training and team development [23, 30].

Predicting group behavior poses fundamental challenges that distinguish it from individual activity recognition. Groups exhibit emergent coordination patterns, such as turn-taking shifts, attention reallocations, spatial regrouping, that cannot be inferred from individual behaviors alone [30, 37]. A person who typically speaks frequently may remain silent when another group member dominates the conversation. Spatial proximity patterns shift dynamically based on task phase and social roles. These structural dependencies require models that reason about *relational context*: not just what each person does, but how their behaviors interconnect within the group’s evolving social dynamics.

Traditional statistical models struggle with this complexity. Our experiments reveal that LSTM models, even when provided with comprehensive contextual features including individual behavioral profiles, network structural metrics, and temporal phase information, plateau at 29% prediction accuracy regardless of context richness. This *context plateau effect* demonstrates an architectural limitation: recurrent neural networks lack the semantic reasoning capacity to interpret how behavioral clusters (“frequent talker”), network properties (“centralized conversation”), and temporal phases (“active collaboration”) interact to shape future group dynamics. Statistical models optimize for element-wise prediction accuracy, achieving 95% by exploiting temporal autocorrelation, yet exhibit only 6% structural similarity to ground truth coordination patterns showing that it completely missing turn-taking changes and attention shifts that characterize meaningful group behavior.

We present **M-CALLM** (Multi-level Context-Aware LLM), a system that transforms raw MR sensor streams (gaze vectors, audio, head/hand positions) into sociogram predictions via hierarchical context encoding and LLM-based forecasting. The system operates in two modes: *intervention mode* predicts the next 32-second window for real-time feedback systems, while *simulation mode* performs autoregressive multi-step prediction for long-horizon team simulation. We evaluate three LLM paradigms spanning the adaptation spectrum: zero-shot prompting tests whether pre-trained models possess sufficient social reasoning capabilities without task examples, few-shot in-context learning ($k = 1$) provides demonstration examples to ground predictions, and supervised fine-tuning with LoRA adapts Gemma-2B (2.6B parameters) using 402 training examples from 12 collaborative groups.

Our evaluation on 16 groups (64 participants, 447 analysis windows spanning ~25 hours) reveals that LLMs achieve **3.2 \times improvement** over statistical baselines when provided with comprehensive context. Supervised fine-tuning reaches 96% structural

similarity for conversation prediction in intervention mode, compared to 30% for context-aware LSTMs. However, results expose critical limitations: (1) *modality-dependent performance*, with excellent conversation modeling but complete failure on rare shared attention events (0% recall due to 1:200 class imbalance), (2) *simulation mode degradation*, where cascading prediction errors cause 83% performance drop as predicted sociograms feed back as context, and (3) *minimal few-shot benefit*, with random example selection performing comparably to sophisticated retrieval strategies (0.5% difference), suggesting LLMs extract reasoning patterns from any contextually appropriate demonstration.

Contributions. This work makes three primary contributions to mobile and ubiquitous sensing systems:

- (1) **System:** We design the first LLM-based pipeline for group behavior prediction from multimodal MR sensors, achieving sub-35ms latency with 7.6 \times richer context than minimal baselines on consumer hardware.
- (2) **Evaluation:** We systematically compare statistical and LLM-based approaches, revealing the *context plateau* (statistical models plateau at 29% regardless of context), *accuracy-similarity gap* (95% accuracy but 6% structural similarity), and *cascading error brittleness* (83% degradation in autoregressive mode).
- (3) **Insights:** Our ablation studies show conversation prediction depends on temporal context (>90% accuracy), proximity on group structure (+6%), while shared attention requires richer visual features, informing sensor prioritization for collaborative systems.

The remainder of this paper surveys related work (Section 2), details our sensing pipeline and context encoding framework (Section 3), evaluates statistical and LLM-based approaches with systematic ablations (Section 4), and discusses implications and limitations (Section 5, 6).

2 Related Work

This paper sits at the intersection of mobile and ubiquitous computing, social sensing, and machine learning. Hence, the related work is structured across core domains: the foundational sensing systems, the architectures for context-aware prediction, and recent advancements in LLM-driven modeling.

2.1 Social Behavior Sensing in Wearable/Mobile Systems

Early mobile sensing systems demonstrated the potential of commodity devices for automatic behavior recognition, moving beyond manual self-reporting through integrated accelerometer, acoustic, and location sensing [26, 27, 31]. Sociometric badges extended these capabilities to group contexts, capturing interaction patterns that correlate with team performance and social dynamics [19, 33]. Building on this foundation, TeamSense demonstrated long-duration prediction of affect states and group cohesion from dyadic interaction features extracted from body-worn sensors [53]. More recent work integrates diverse sensing modalities including capacitive, acoustic, and physiological signals [1, 3, 25], though primarily for recognition rather than prediction. The sensor-in-the-loop paradigm shows how LLMs can leverage sensor-derived context for personalized individual responses [40], but this work targets single users rather

than collaborative groups. As collaboration shifts to mixed reality environments [2, 5, 42], new sensing opportunities emerge, yet group-level behavioral forecasting remains largely unexplored.

2.2 Computational Models for Behavior Prediction

Sequential models, such as Recurrent Neural Networks (RNNs) and Long Short-Term Memory (LSTMs) have been widely applied to behavioral prediction tasks, from activity recognition to routine modeling [12, 34, 36]. Hybrid architectures incorporating attention mechanisms further improved performance by learning both spatial and temporal features [28, 47], though these statistical approaches rely on numerical feature engineering and struggle with semantic context or complex social dynamics.

Recent work explores LLMs for temporal prediction, leveraging their semantic reasoning capabilities. Time-LLM [16] combines temporal embeddings with parameter-efficient fine-tuning for time series forecasting, while approaches like LAMP demonstrate few-shot causal reasoning for event sequences [44].

In contrast, while these approaches excel in text-based or simulated environments, their effectiveness for multimodal group behavior in physical and MR settings, where visual attention, spatial proximity, and embodied cues shape dynamics, remains unvalidated. Our work addresses this gap by grounding LLM-based behavior modeling in real sensor data from collaborative MR tasks.

2.3 Context-Aware Systems

Context-aware computing established frameworks for systems that adapt based on location, identity, activity, and temporal information [8, 9]. Early mobile systems demonstrated context inference from sensor data [10, 11, 31], with large-scale studies like LiveLab providing longitudinal measurements of smartphone usage in natural settings [43]. However, traditional approaches rely on hand-crafted rules mapping contextual inputs to system responses, struggling with ambiguous information and complex relationships in dynamic social environments.

For group behavior modeling, context spans multiple hierarchical levels: individual traits capturing stable behavioral patterns [41], group structure quantifying network properties like reciprocity and centralization [18], and temporal phases identifying distinct collaboration stages [42]. While traditional machine learning treats context as fixed feature vectors, integrating these multi-level contexts into flexible predictive models remains challenging. In contrast, our work encodes individual patterns, group structure, and temporal phases as natural language context, enabling LLMs to leverage semantic reasoning about how contextual factors interact in MR collaboration tasks.

2.4 LLM-Based Agent Systems

Generative agents powered by LLMs have demonstrated emergent social behaviors in simulated environments. Park et al. [35] showed that agents equipped with memory, reflection, and planning mechanisms produce realistic relationship formation, information diffusion, and coordinated activities over extended periods. Multi-agent

frameworks extend these capabilities to model cooperation in social dilemmas [38] and competitive dynamics [54], revealing both potential and limitations of LLM-based collective decision-making.

These systems leverage various adaptation strategies. Zero-shot prompting provides task descriptions based solely on pre-training knowledge [20], while few-shot learning supplies examples to guide behavior [4]. Chain-of-thought prompting enhances reasoning through step-by-step explanations [50], and parameter-efficient methods like LoRA [13] enable task-specific fine-tuning with minimal computational overhead.

Unlike rule-based systems that map fixed feature vectors to responses, our work encodes hierarchical context as natural language, enabling LLMs to reason dynamically about how individual patterns, group structure, and temporal phases interact during MR collaboration for a holistic group behavior modeling and prediction.

3 System Architecture and Evaluation Approach

This section presents **M-CALLM**’s architecture for LLM-based group behavior prediction and our evaluation methodology. The designed framework transforms raw, time-series sensor data from a collaborative MR environment into a structured linguistic context for a LLM to perform group behavior prediction. We emphasize the system’s ability to capture the complex social dynamics and structural group coordination and not merely individual context that traditional statistical models fail to model effectively. Our complete framework is shown in Figure 2.

3.1 Data Collection and System Setup

To rigorously evaluate context-aware group behavior prediction, we deployed a dedicated multimodal sensing system within a controlled collaborative MR setting.

The study involved 64 participants (age 21-42, mean 24) in 16 groups of 4, using Meta Quest Pro headsets for a collaborative image sorting task as a representative for collaboration task [52]. To minimize the potential effect of differing MR experience levels on task performance and behavior, all participants completed a tutorial session prior to the main task to familiarize themselves with MR mechanics. Participants categorized 28 OASIS dataset images into six emotion categories, designed to encourage decision-making, communication, and social coordination without time limits [21, 52]. The IRB-approved study, with participants’ informed oral consent, aimed to observe open collaboration in MR, focusing on interaction, task performance, and subjective experiences to analyze group behavior and validate the proposed system.

Our setup utilizes the MR headsets instrumented to capture four primary channels of raw sensor data from the 64 participants forming 16 distinct groups:

- (1) **Gaze & Attention (S_g)**: Raw gaze vectors, derived from eye-tracking sensors, processed into metrics of shared attention (i.e., when two or more individuals are fixating on the same real-world or virtual object) [32, 48].
- (2) **Audio & Conversation (S_a)**: Continuous audio streams, processed to identify speaker turns, speaker diarization, and turn-taking duration.

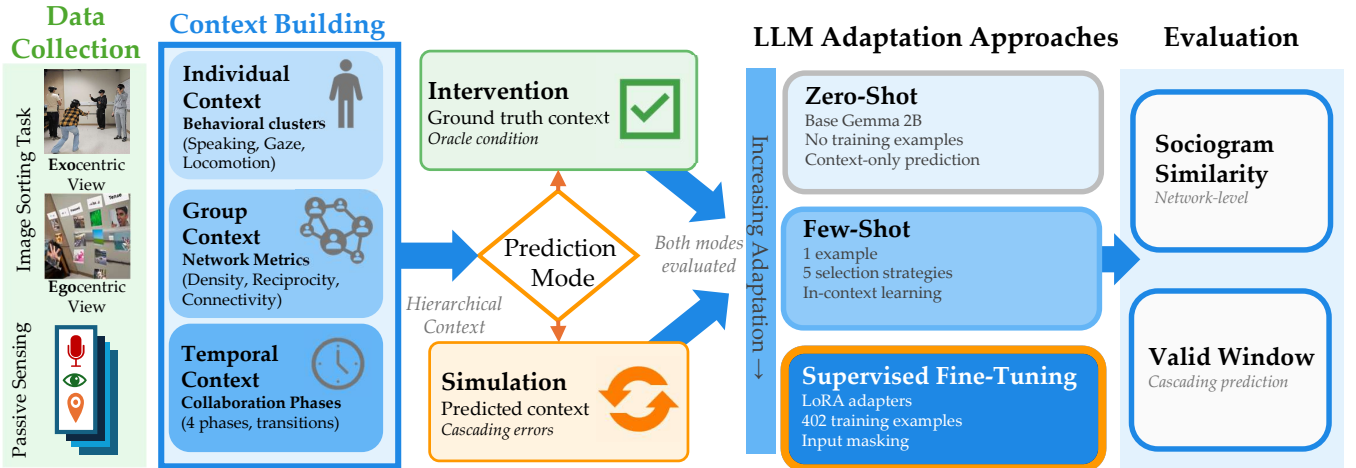


Figure 2: Context-aware LLM system architecture. Multimodal MR sensor data (gaze, audio, location, task state) are processed into sociograms representing conversation, proximity, and shared attention networks. Hierarchical context including individual behavioral profiles, group structural properties, and temporal dynamics is encoded as natural language and provided to Gemma-2B for next-window prediction via zero-shot, few-shot ($k = 1$), or fine-tuned (LoRA) approaches. The system achieves sub-35ms TTFT with 7.6x richer context than minimal baselines, enabling real-time deployment on consumer hardware.

- (3) **Location & Proximity (S_p):** Relative head and hand positions, used to compute inter-personal distance and spatial grouping.
- (4) **Task State (S_t):** Log data tracking progress on the collaborative task, providing task context.

All sensor data is synchronized and segmented into fixed-length, T-second observation windows (e.g., 32-second windows as discussed in the Section 3.6). The system processes the raw streams (S_g, S_a, S_p) for each participant i and group G into a set of structured, numerical features, serving as the input for the subsequent representation and modeling stages.

3.2 Group Behavior Representation (Sociograms)

Instead of predicting low-level sensor values, the goal of our system is to predict structural group coordination. We represent this coordination state at time t as a set of time-evolving, directed, and weighted Sociograms, G_t , where nodes represent individuals and edges represent the strength of a specific interaction type. The prediction target is the sociogram state in the next window, G_{t+1} . This makes the problem an explicit sociogram prediction task where the LLM’s role is to predict pairwise interactions that determine the network structure and edge weights.

Specifically, for each time window ($T = 32$ seconds), we construct three concurrent Sociograms for each group G in window t :

- (1) **Conversation Sociogram G^{conv} :** is a directed graph where the edge weight $w_{i,j}$ represents the normalized amount of speaking time person i directed toward person j .
- (2) **Proximity Sociogram G^{prox} :** is an undirected graph where the edge weight $w_{i,j}$ represents the total duration person i spent in close-proximity threshold (e.g., 1.5 ft) of person j [46].

- (3) **Shared Attention Sociogram G^{att} :** is an undirected graph where the edge weight $w_{i,j}$ represents the duration with which person i shared attention on the same object or area as person j . The combined set $\{G^{\text{conv}}, G^{\text{prox}}, G^{\text{att}}\}$ forms the ground-truth target for the LLM’s prediction. This structural perspective is critical because prediction models can achieve high element-wise accuracy by predicting individual behaviors while missing important coordination patterns, such as turn-taking shifts, attention reallocations, or subgroup formations (as will be discussed in the Evaluation Section 4.1.1).

3.3 Multi-Level Context Encoding

Our Multi-level Context Aware LLM (M-CALLM) framework’s core architectural innovation is the serialization of multi-modal, network-level context into Natural Language (NL) prompts, allowing LLMs to leverage their semantic and causal reasoning capabilities. The LLM predicts the next set of sociograms G_{t+1} based on three distinct levels of context from the current window t .

- (1) **Individual Behavioral Profiles:** C_t^{indiv} The intuition is to capture stable individual traits.
 - **Content:** For each individual $i \in G$, we calculate and serialize key behavioral metrics, such as speaking time ratio, average distance to group centroid, and attention distribution entropy. We encode stable behavioral traits using MoCoMR clustering [41], which performs unsupervised Gaussian Mixture Model (GMM) analysis of speaking frequency (utterances per session), gaze patterns (target distribution), and locomotion dynamics (speed, path entropy). Each participant is assigned to behavioral clusters with natural language descriptors (e.g., “frequent talker,” “high gaze activity,” “dynamic mover”). These cluster assignments are computed once per session based on full-session statistics and remain

constant across all prediction windows, providing LLMs with persistent individual characteristics.

- **Serialization Example:** “Participant A’s profile: Frequent Talker (119 utterances/session), High Gaze Activity (2014 instances/session), Highest Dynamic movement (hightortuosity and speed).”

(2) **Group Structural Properties** C_t^{group} : The intuition is to capture the dynamic group structure.

- **Content:** This represents the global, network-level state of the group’s current Sociograms ($\{G^{\text{conv}}, G^{\text{prox}}, G^{\text{att}}\}$). For each context window $T = 32$ second, we extract density ρ , reciprocity, eigenvector centrality, and clustering coefficients across the three modality networks [30, 49]. These metrics are combined via PCA-weighted fusion [41], where each modality’s contribution is weighted by its explained variance ratio from PCA of the metric covariance matrix, producing a unified structural representation that adapts to current coordination patterns.
- **Serialization Example:** “Conversation network: density=0.35, reciprocity=0.42. Proximity network: density=0.28, clustering=0.31. Fused network: density=0.42, reciprocity=0.58.”

(3) **Temporal Dynamics** C_t^{temp} : The intuition is to capture longitudinal awareness of the group behavior. This allows the LLM to infer change rates.

- **Content:** We use unsupervised deep clustering of temporal phases using MURMR [42], which segments sessions into collaboration phases (e.g., exploration, active discussion, consensus) via variational autoencoder embeddings. Each window includes: (1) the current phase identifier, (2) phase-level aggregated metrics (speaking entropy, joint attention event counts), and (3) phase stability (consecutive windows in current phase). In addition, we include a five sliding-window interaction history $\{G_{t-5:t-1}^{\text{conv}}, G_{t-5:t-1}^{\text{prox}}, G_{t-5:t-1}^{\text{att}}\}$ to capture short-term trends in turn-taking and attention shifts. The 5-window span (2.67 minutes) is grounded in time series forecasting research showing optimal performance when input window length approximates the forecast horizon [17], and in conversation analysis demonstrating that this duration captures approximately 48 conversational turns (given mean turn durations of 1.68 seconds [24]) while falling within the “seconds to minutes” range where humans naturally track temporal patterns in social interactions [23].
- **Serialization Example:** “Phase: Animated Collaboration (Cluster 1), duration: 5 consecutive windows. Structural trends: Density increasing (0.15 to 0.22), Reciprocity increasing (0.33 to 0.50).”

This hierarchical structure enables LLMs to integrate persistent traits (C_t^{indiv}), dynamic network structure (C_t^{group}), and temporal evolution (C_t^{temp}) when predicting future interactions. Context is serialized as structured natural language prompts that balance human interpretability with computational precision, as illustrated in Table 1.

3.4 LLM-Based Prediction Pipeline

M-CALLM employs LLM as semantic reasoning engines for group behavior prediction, transforming serialized multi-level context into

Table 1: Example multi-level context for a prediction window. Individual clusters remain constant; group and temporal contexts update every $T = 32$ seconds.

Context Level	Representation
Individual	Speaking: Frequent Talker (Cluster 0, 119/session) Gaze: High Activity (Cluster 2, diverse focus) Locomotion: Dynamic (Cluster 2, high speed)
Group	Conversation: $\rho = 0.35$, reciprocity=0.42 Proximity: $\rho = 0.28$, clustering=0.31 Shared Attention: $\rho = 0.15$, clustering=0.09
Temporal	Phase: Animated Collaboration (Cluster 1) Duration: 5 consecutive windows Trends: Density \uparrow (0.15→0.22), Reciprocity \uparrow (0.33→0.50)

structured sociogram forecasts. The system architecture supports three LLM paradigms with distinct adaptation strategies, zero-shot, in-context learning, and supervised fine-tuning and two deployment modes with complementary evaluation objectives.

3.4.1 Prompt Structure and Output Format. The complete prompt P_t consists of six structured components rendered via Jinja2 templates:

$$P_t = [I \mid C_t^{\text{temp}} \mid C_t^{\text{indiv}} \mid C_t^{\text{group}} \mid H_t^{\text{pair}} \mid E_t^{\text{event}} \mid \text{FMT}]$$

comprising: (1) task instructions I , (2) temporal context C_t^{temp} (phase, stability, trends), (3) individual profiles C_t^{indiv} (MoCoMR clusters [41]), (4) group structural metrics C_t^{group} (density, reciprocity, centrality, clustering), (5) pairwise interaction history H_t^{pair} (last 5 windows), (6) event timeline E_t^{event} (last 10 windows), and (7) output format FMT as illustrated in Figure 3.

The LLM generates timestep-by-timestep binary predictions in structured text format. For each participant pair and each second $s \in [t+1, t+32]$, the model predicts three binary interaction indicators using the notation $t=s$: $C=[Y/N]$, $P=[Y/N]$, $S=[Y/N]$, where C, P, and S denote conversation, proximity, and shared attention, respectively. A robust parsing system (ResponseParser) extracts these predictions using pattern matching with multiple fallback strategies to handle output variability, converting text responses into binary adjacency matrices $G_{t+1} = \{G_{t+1}^{\text{conv}}, G_{t+1}^{\text{prox}}, G_{t+1}^{\text{attn}}\}$ for quantitative evaluation.

3.4.2 Inference Modes. The framework supports two complementary deployment modes that test distinct system capabilities:

- (1) **Intervention Mode (Oracle Context):** Single-step prediction $G_t \rightarrow G_{t+1}$ where each window receives ground truth context from sensors. This mode evaluates the LLM’s semantic reasoning capacity under ideal conditions, suitable for real-time intervention systems that provide immediate feedback based on current sensor observations.

(2) **Simulation Mode (Cascading Predictions):** Autoregressive multi-step prediction $G_t \rightarrow G_{t+1} \rightarrow G_{t+2} \rightarrow \dots$ where predicted sociograms are parsed, converted to pseudo-features (via `simulation_context_builder.py`), and fed back as context for subsequent predictions. This mode tests robustness to compounding errors over extended horizons, enabling long-term team behavior simulation without continuous sensor access.

The key distinction is context source: intervention mode uses *ground truth* features at every timestep (testing reasoning capacity), while simulation mode uses *predicted* features after the first window (testing error propagation resilience).

3.4.3 LLM Adaptation Paradigms. We evaluate three configurations spanning the spectrum from zero-parameter adaptation to full supervised fine-tuning:

(1) **Zero-Shot Prompting.** Gemma-2B-IT receives structured task descriptions and multi-level context serialized as natural language (prompt length: $\sim 4,200$ tokens) without any task-specific training examples. This tests whether pre-trained models possess sufficient world knowledge about social dynamics to perform group behavior reasoning through prompt engineering alone. An example of the prompt is shown in Figure 3.

(2) **Few-Shot In-Context Learning ($k = 1$).** The zero-shot prompt is augmented with a single demonstration example showing complete input-output mapping from context to sociogram predictions (adds $\sim 4,552$ tokens per example). We focus on $k = 1$ due to Gemma-2B’s 8,192-token context limit, which constrains the number of demonstrations that can be included alongside full multi-level context.

We compare three example selection strategies: (1) *random sampling* from the training pool as an unbiased baseline with $O(1)$ computational complexity, (2) *phase-similar selection* using cosine similarity in MURMUR’s temporal phase embedding space (128-dimensional VAE latents [42]) to retrieve contextually relevant examples with $O(N \log N)$ overhead, and (3) *diversity-based selection* via k-means++ initialization to maximize coverage of interaction patterns with $O(N^2)$ complexity. Examples are selected from other groups (excluding the current test group) to ensure demonstrations come from different participants while maintaining similar interaction contexts. The sample of a prompt with a provided example can be seen in Figure 3.

(3) **Supervised Fine-Tuning (SFT).** Gemma-2B is adapted using LoRA [14] with rank $r = 16$, scaling factor $\alpha = 32$, and 5% dropout, following recommended configurations for 2B-scale models. We target query, value, and output projection matrices (`q_proj`, `v_proj`, `o_proj`) in the attention mechanism, freezing all other parameters. This yields 2.5M trainable parameters (0.10% of the base model’s 2.6B).

Training uses Groups 1-12 (402 windows from 90/10 train/val split) for 3 epochs with AdamW optimizer (learning rate 10^{-4} , effective batch size 8 via gradient accumulation, 10% linear warmup). Maximum sequence length is set to 8,192 tokens to accommodate full multi-level context plus complete 6-pair predictions. Critically, we apply causal attention masking to compute cross-entropy loss *only on generated prediction tokens*, excluding input context from loss calculation. This forces the

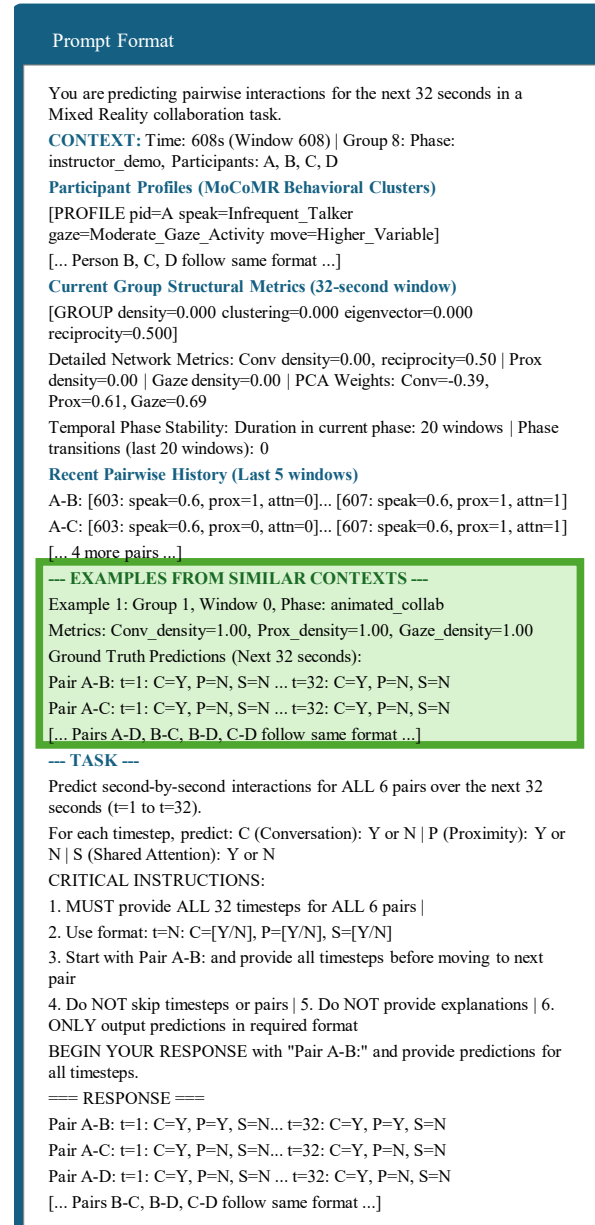


Figure 3: Prompt structure for group interaction prediction. Key components include participant behavioral profiles, group structural metrics, network metrics with PCA weights, temporal phase stability, recent pairwise history, few-shot examples (highlighted in green), and task instructions. The example section (green) is omitted in the zero-shot condition.

model to learn context-to-prediction mapping rather than input reconstruction.

Table 2: Mapping Team Science Constructs to M-CALLM framework Components.

IPO Component	Description		Technical Operationalization
Input	Static team composition and task characteristics.		Initial features and contextual metrics within C_t^{indiv} .
Process (Quantified SMM)	The observable and unobservable team interactions, which facilitate coordination and adaptation.		Sociograms (G_t) and the Multi-Level Context Encoding ($C_t^{\text{temp}}, C_t^{\text{indiv}}, C_t^{\text{group}}$).
Output	Observable task results and emergent structural states.		The predicted Sociogram (G_{t+1}) and the task performance metrics (e.g., time to completion).

3.5 Theoretical Framing: Operationalizing the IPO Model

Our M-CALLM framework is explicitly structured to operationalize the well-established **Input-Process-Output (IPO) Model** of team effectiveness [15] and the **Shared Mental Model (SMM)** framework [29]. We map our system components to these constructs, thereby validating our technical design choices through established team science theory as summarized in Table 2.

- (1) **Input Component (Initial Conditions):** This is operationalized by the static team characteristics and task constraints of the collaborative MR environment (e.g., card sorting game complexity). These initial conditions, such as participant composition and task parameters, are captured as static features in the LLM’s initial context and in the running measure of disposition provided by the **Individual Behavioral Profiles** (C_t^{indiv}).
- (2) **Process Component (Quantified SMM):** This is the technical focus of our system. The “Process” component, representing the team’s ongoing interaction, coordination, and the SMM in-action, is quantitatively captured by the three concurrent Sociograms $G_t = [G_t^{\text{conv}}, G_t^{\text{prox}}, G_t^{\text{att}}]$ defined in Section 3.2.
 - **Direct SMM Measurement:** The structure of G_t (e.g., density in G^{att} , centralization in G^{conv}) can provide an objective, real-time measure of the team’s coordination effectiveness [7].
 - **Context for Reasoning:** The **Group Structural Properties** (C_t^{group}) and **Temporal Dynamics** (C_t^{temp}) derived from G_t are serialized into the LLM prompt, forcing the model to reason about the complex, non-linear dependencies inherent in human team process, thus overcoming the **Context Plateau** of statistical models as will be discussed in Section 4.1.2.
- (3) **Output Component (Predicted State):** The prediction target is the future Process state, G_{t+1} . This predicted Sociogram represents the anticipated **emergent structural coordination** of the team in the next time window. This predicted output directly enables both application modes (intervention and simulation).

3.6 Evaluation Protocol

Having defined the system architecture, LLM adaptation paradigms, and theoretical grounding, we now describe our comprehensive evaluation methodology.

3.6.1 Dataset and Experimental Design. Our evaluation uses data from the 16 groups of 4 participants described in Section 3.1. Sessions range from 4.8 to 18.4 minutes (mean: 9.7 minutes), segmented into 32-second analysis windows with 16-second stride, yielding 447 total windows across all groups (distribution: 18-69 windows per group, ~25 hours total interaction time).

We employ different evaluation strategies based on model training requirements:

- **Prompting Approaches (Zero-Shot, Few-Shot):** Evaluated on all 16 groups since these approaches require no training data. For few-shot in-context learning, demonstration examples ($k = 1$) are selected from other groups in the dataset (excluding the current test group), ensuring examples come from different participants while maintaining similar interaction contexts based on the selection strategy (random, phase-similar, or diversity-based).
- **Supervised Fine-Tuning (SFT):** Trained on Groups 1-12 (402 windows with 90/10 train/validation split), evaluated on held-out Groups 13-16 to assess generalization to completely unseen participants and interaction patterns. This split ensures test performance reflects the model’s ability to reason about novel group dynamics rather than memorizing training participants.
- **Context Ablation Study:** Conducted on a single representative group to isolate the contribution of individual context components (temporal, individual, group) to prediction accuracy across modalities. Group selection based on median session length and balanced interaction patterns.

All three LLM paradigms are evaluated under both intervention mode (oracle ground truth context) and simulation mode (cascading predictions with context feedback), yielding six experimental configurations.

3.6.2 Baseline Methods. We compare LLM approaches against two baseline categories:

Simple Baselines. Three non-parametric methods establish lower bounds:

- **Persistence:** Repeats last observed sociogram, testing whether temporal autocorrelation alone enables prediction.
- **Temporal Smoothing ($N \in \{3, 5\}$):** Averages previous N sociograms, providing basic regularization against abrupt transitions.
- **Stratified Random Sampling:** Generates sociograms by sampling edge probabilities matched to empirical interaction rates per modality, testing whether base rate information suffices.

Statistical Baseline (LSTM + Full Context). Bidirectional LSTM encoder-decoder architecture (2048 hidden units) with attention mechanism over individual behavioral profiles and group

network metrics. This parametric baseline leverages the same multi-level context as LLM approaches (individual profiles, group structure, temporal phases) but uses continuous feature vectors instead of natural language serialization. Trained for 30 epochs with Adam optimizer on Groups 1-12, evaluated on Groups 13-16.

3.6.3 Evaluation Metrics. We evaluate prediction quality using one primary metric that captures structural coordination patterns and two secondary metrics that assess temporal stability and network property preservation.

Primary Metric: Sociogram Similarity. We measure weighted Jaccard similarity between predicted and ground truth sociograms for each 32-second window. Unlike element-wise accuracy which treats each pairwise interaction independently, sociogram similarity captures emergent group-level coordination patterns including turn-taking shifts, attention reallocations, and spatial regrouping [30, 37]. For each modality $m \in \{\text{conv, prox, attn}\}$, we compute weighted Jaccard between predicted adjacency matrix \hat{A}_t^m and ground truth A_t^m , then report per-modality similarities and their average.

As we demonstrate in Section 4.1.1, persistence baselines achieve 95% pairwise accuracy while exhibiting only 6% sociogram similarity, completely missing coordination changes. This accuracy-similarity gap motivates our use of structural metrics as the primary evaluation criterion.

Secondary Metrics. We employ two complementary metrics to assess prediction quality beyond aggregate similarity:

- *Valid Window Rate:* Proportion of windows achieving $\geq 80\%$ mean accuracy across conversation and proximity predictions. This metric assesses temporal stability in simulation mode, where cascading errors may degrade window-level performance despite reasonable aggregate similarity.
- *Network Property Preservation:* Pearson correlation between predicted and ground truth network metrics (density, reciprocity, clustering coefficient). This evaluates whether models capture higher-order structural patterns beyond edge-level accuracy, measuring how well predictions preserve global network characteristics.

4 Experimental Evaluation

This section presents a comprehensive evaluation of context-aware group behavior modeling, comparing statistical baselines against LLM-based approaches. We design experiments to: (i) demonstrate the fundamental limitations of statistical models when modeling group coordination, and (ii) assess how effectively LLMs leverage multi-level context to capture group dynamics.

4.1 Limitations of Statistical Models

We conducted extensive evaluation to establish the capabilities and fundamental limitations of statistical approaches across three progressive stages: individual-level models, group-level models without explicit context, and context-aware models with hierarchical information. These experiments motivate our LLM-based approach by demonstrating that statistical models hit an architectural ceiling regardless of context complexity.

Table 3: Persistence Baseline: High Accuracy but Poor Structure Preservation. Persistence achieves strong element-wise metrics (F1, balanced accuracy) by exploiting temporal autocorrelation, but exhibits poor sociogram similarity due to failure in capturing coordination changes.

Metric	Conv.	Prox.	Att.	Overall
F1 Score	0.984	0.896	0.936	0.955
Balanced Accuracy	0.486	0.916	0.941	0.949
MCC	-0.008	0.840	0.887	0.891
<i>Sociogram Similarity (Weighted Jaccard)</i>				
Intervention Mode	0.068	0.045	0.074	0.062

4.1.1 The Persistence Problem: Why Accuracy is Insufficient. Before evaluating complex models, we first demonstrate why element-wise accuracy is an insufficient metric for group coordination prediction. Simple persistence baseline (repeating the last observed sociogram state) achieves deceptively high element-wise accuracy by exploiting temporal autocorrelation in individual behaviors. However, this high accuracy masks complete failure to capture group coordination dynamics.

The stark contrast between element-wise and structural metrics (Table 3) reveals the fundamental limitation of accuracy-based evaluation. Persistence achieves $F1 > 0.89$ across all modalities and 0.955 overall, with Matthews correlation coefficient (MCC) of 0.891 indicating strong correlation with ground truth interaction patterns. However, sociogram similarity remains extremely low (0.062), demonstrating complete failure to capture coordination dynamics.

This accuracy-similarity gap arises because persistence correctly predicts the majority class (no interaction) for most pairs due to high temporal autocorrelation ($\rho \approx 0.53\text{-}0.73$ across modalities), but fails catastrophically when coordination patterns change. For example, when the group transitions from exploration to active discussion, persistence continues predicting dispersed proximity patterns while ground truth shows spatial clustering around a focal participant. The model achieves high recall (0.939) by repeating previous interactions, but completely misses turn-taking shifts, attention reallocations, and spatial regrouping that characterize meaningful coordination dynamics.

Notably, conversation exhibits paradoxically high F1 (0.984) but near-zero MCC (-0.008) and extremely low balanced accuracy (0.486). This occurs because 99.76% of conversation pairs are active in the data (extreme class imbalance), and persistence trivially predicts "conversation present" for nearly all pairs, achieving 99.8% precision and 97.2% recall. However, the model never correctly identifies the absence of conversation (TN=0 in confusion matrix), resulting in random-level performance for the negative class. **This motivates our use of sociogram similarity rather than element-wise accuracy as the primary evaluation metric**, as only structural metrics capture whether models learn coordination dynamics versus exploiting class imbalance in individual behaviors.

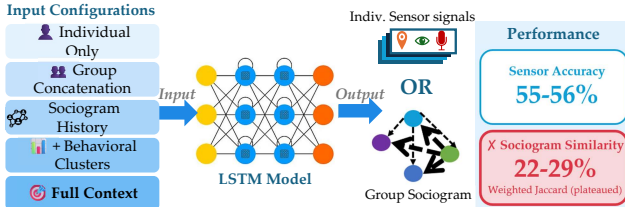


Figure 4: Statistical model context plateau. LSTM performance remains constant (~29% sociogram similarity) across four context configurations: individual-only, individual+group, individual+temporal, and full multi-level context. While sensor-level accuracy improves with richer context (left), sociogram similarity does not (right), revealing statistical models’ inability to capture emergent coordination patterns.

Table 4: LSTM performance across context configurations. Despite increasing context complexity, weighted Jaccard similarity plateaus around 29% (<2% variation), demonstrating architectural limitation rather than insufficient context.

Context Configuration	Overall WJ	Δ from Individual
Individual Only	29.3%	—
Group (Concatenated)	29.1%	-0.2%
Group + Sociogram History	28.2%	-1.1%
Group + Behavioral Clusters	29.1%	-0.2%
Full Context	28.7%	-0.6%
Range (max - min)	1.1%	

4.1.2 The Context Plateau: Statistical Models Cannot Leverage Rich Context. To systematically evaluate whether statistical models can leverage hierarchical contextual information, we trained LSTM models across five context configurations of increasing complexity: (1) individual features only, (2) group concatenation (all members’ features), (3) group + sociogram structure (previous edge weights), (4) group + behavioral clusters (GMM-derived profiles), and (5) full context (sociogram + clusters + temporal phases). Each model uses identical architecture (2048 hidden units, Adam optimizer, 30 epochs) with only context features varied.

Results reveal a striking pattern (Figure 4): **performance plateaus at approximately 29% weighted Jaccard regardless of context complexity**, with less than 2% variation across all five configurations (Table 4).

Critically, this plateau occurs despite models achieving 55-56% training accuracy on raw sensor predictions (Table 5, and Figure 5), revealing an **accuracy-similarity gap** analogous to but distinct from the persistence problem: models optimize for individual sensor prediction without preserving group coordination structure. The <2% variation across configurations indicates that the performance bottleneck stems from architectural limitations in reasoning capacity rather than insufficient contextual information.

Implications. These results establish two fundamental limitations of statistical approaches to group behavior modeling. First, the

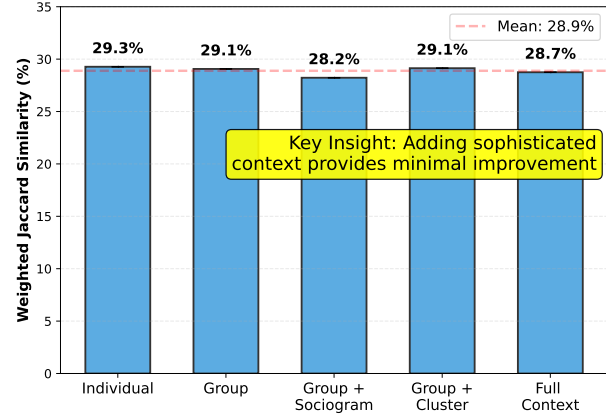


Figure 5: LSTM weighted Jaccard across context configurations. Performance plateaus around 29% regardless of context complexity. The flat trend demonstrates architectural limitations: statistical models cannot leverage rich contextual information to improve group coordination prediction.

Table 5: Context encoding experiments: Training accuracy vs. sociogram similarity. Despite achieving 55-56% training accuracy, all experiments plateau at 22-23% weighted Jaccard similarity, demonstrating the accuracy-similarity gap.

Experiment	Train Acc	WJ Sim	Conv	Prox	Att
A: Sociogram Context	55.2%	22.4%	29.4%	21.6%	16.1%
B: Cluster Context	55.5%	22.1%	26.8%	22.6%	17.0%
C: Both Contexts	56.3%	23.1%	29.8%	21.5%	18.0%

context plateau effect demonstrates that statistical models cannot effectively leverage rich contextual information—performance remains constrained at approximately 29% weighted Jaccard regardless of whether models receive individual features, group structure, behavioral semantics, or comprehensive hierarchical context. Second, the **accuracy-similarity gap** reveals that high training accuracy (55%) on individual sensor predictions does not translate to successful group coordination capture (23% similarity), indicating that sensor-level prediction accuracy is insufficient to ensure structural understanding of social dynamics.

These findings demonstrate that the limitation is not insufficient data or context, but rather an architectural constraint: LSTMs lack the semantic reasoning capabilities to interpret complex social coordination patterns such as turn-taking dynamics, role-based behaviors, and attention reallocation mechanisms. This motivates our investigation of LLM-based approaches that can leverage natural language representations of hierarchical context.

4.2 LLM Performance: Breaking Through the Ceiling

Having established that statistical models plateau at 29% regardless of context, we now evaluate whether LLMs can break through this ceiling by leveraging semantic reasoning over hierarchical behavioral context. We compare three LLM configurations: zero-shot prompting (no task-specific training), few-shot in-context learning ($k=1$ demonstration), and supervised fine-tuning (SFT) with LoRA adaptation.

4.2.1 Main Results: Intervention Mode. Table 6 presents sociogram similarity across all methods in intervention mode, where models receive ground truth context. The results demonstrate that **LLMs achieve 3.2x improvement over statistical baselines**, with SFT reaching 96% weighted Jaccard for conversation prediction compared to 29.8% for LSTM with full context.

The results reveal several key findings. First, FT achieves 0.958 weighted Jaccard for conversation prediction—96% structural similarity to ground truth—compared to LSTM’s 0.298 (29.8%), representing a **3.2x improvement**. This dramatic gap demonstrates that LLMs can capture coordination patterns statistical models fundamentally cannot.

Second, **few-shot exhibits strong performance** with phase-similar examples achieving 0.582 average similarity without task-specific training, outperforming the LSTM baseline (0.231). The substantial improvement over zero-shot performance (0.101) indicates that in-context learning can effectively ground the model’s pre-trained knowledge for this task.

Third, **SFT exhibits strong modality-dependent specialization**, near-optimal conversation prediction (0.958) but weak proximity modeling (0.104). This asymmetry likely reflects the model’s capacity to capture semantic coordination patterns while struggling with spatial interactions that may be better represented through continuous features rather than discrete linguistic tokens.

Finally, **zero-shot prompting underperforms all baselines**, confirming that generic pre-trained knowledge is insufficient for modeling task-specific group dynamics without appropriate contextualization.

4.2.2 Computational Efficiency Analysis. A critical question for practical deployment is whether the 3.2x performance improvement comes at prohibitive computational cost. We evaluate inference efficiency across four context complexity levels (minimal to full hierarchical context) on an NVIDIA RTX 4060 Ti GPU (16GB VRAM, consumer-grade hardware).

Key Finding: Negligible Overhead. Despite processing 7.6x richer contextual information (237 to 1,799 characters), our system achieves *faster* inference (Table 7): time-to-first-token (TTFT) decreases by 3.6% (33.4ms to 32.1ms), total inference time decreases by 19.7% (4.15s to 3.33s), and throughput increases by 3.3% (30.2 to 31.2 tokens/s). Memory consumption scales sub-linearly, increasing by only 0.7% (5.02GB to 5.05GB). All context configurations maintain TTFT below 35ms, meeting latency requirements for real-time interactive systems. The details of the overhead analysis is presented in Table 8.

Scalability Validation. To assess performance beyond our experimental configurations, we tested five context lengths spanning

237 to 3,328 characters (14x range). Inference time exhibited sub-linear scaling: total time varied between 2.73s and 4.37s despite the 14-fold context increase, TTFT remained remarkably stable (32-34ms), and throughput fluctuated within a narrow 6% band (29.3-31.3 tokens/s). This sub-linear scaling behavior indicates efficient attention mechanisms in the Gemma-2 architecture, confirming that context-rich prompts can be deployed without prohibitive computational costs on consumer-grade hardware.

These findings demonstrate that comprehensive behavioral context—spanning individual profiles, group structures, temporal dynamics, and interaction history—can be integrated with negligible computational overhead, enabling real-time deployment of LLM-based group sensing systems.

4.2.3 Simulation Mode: Challenges with Error Propagation. While intervention mode demonstrates strong modeling capability (96% for conversation), simulation mode reveals brittleness to cascading errors. Table 9 presents simulation mode performance where predicted sociograms become context for subsequent predictions.

Cascading Error Problem. Few-shot conversation similarity collapses from 0.785 to 0.007 (99.1% degradation), while SFT degrades from 0.958 to 0.165 (82.8% degradation). This reveals that initial mispredictions produce incorrect density and reciprocity metrics in group context, which bias subsequent predictions toward erroneous interaction patterns. Analysis of temporal dynamics shows immediate collapse: conversation predictions fail by cascade depth 2 (half-life ≤ 2 windows) then stabilize at floor values, indicating binary failure mode (works once, fails thereafter) rather than gradual decay.

Interestingly, proximity predictions remain relatively stable (0.425-0.104), suggesting spatial interactions are less context-dependent and primarily driven by persistent locomotion patterns. However, the stratified random baseline outperforms all LLM methods in simulation mode (0.993 conversation similarity), demonstrating that lack of history dependence prevents error accumulation at the cost of missing temporal dynamics.

Understanding Simulation Mode Failure. The intervention mode results (96% conversation similarity) demonstrate that LLMs can capture group coordination patterns when provided with accurate context. However, simulation mode degradation reveals a critical brittleness: the immediate collapse pattern (half-life ≤ 2 windows) indicates binary failure—the model works once, then fails completely rather than accumulating small errors.

This stems from cascading context corruption. When the model mispredicts conversation edges in window $t+1$, these errors propagate to group structural metrics (density, reciprocity) computed for window $t+2$ ’s context. The LLM, trained to trust context features, generates predictions consistent with erroneous metrics rather than recovering from initial errors. Interestingly, the stratified random baseline outperforms all LLM methods in simulation mode (0.993 vs 0.007-0.165), demonstrating that lack of history dependence prevents error accumulation—though at the cost of completely missing temporal dynamics. This performance inversion highlights a fundamental tradeoff: models leveraging rich context become vulnerable to context corruption, while context-free models remain stable but uninformative.

Table 6: Sociogram similarity in intervention mode. LLM approaches achieve 3.2x improvement over LSTM baseline. Shared attention scores (–) indicate systematic LLM failure (0% recall). Average computed over conversation and proximity only.

Method	Conv Sim	Prox Sim	Att Sim	Avg Sim	vs LSTM
<i>Simple Baselines</i>					
Persistence	0.068	0.045	0.074	0.062	–
Stratified Random	0.044	0.044	0.044	0.044	–
<i>Statistical Model</i>					
LSTM + Full Context	0.298	0.215	0.180	0.231	1.0x
<i>LLM Approaches</i>					
Zero-Shot	0.067	0.188	0.048	0.101	0.4x
Few-Shot (Random, k=1)	0.768	0.477	–	0.579	2.5x
Few-Shot (Similar, k=1)	0.785	0.474	–	0.582	2.5x
Few-Shot (Diverse, k=1)	0.740	0.451	–	0.554	2.4x
SFT (Intervention)	0.958	0.104	–	0.395	3.2x

Table 7: Inference performance across context complexity levels. Despite 7.6x context increase (237 to 1,799 characters), TTFT remains stable (<35ms) and total time decreases by 19.7%. All measurements reported as mean \pm std over 10 runs.

Context Type	Length (chars)	TTFT (ms)	Total (s)	Throughput (tok/s)
Minimal	237	33 \pm 3	4.15 \pm 0.55	30.2 \pm 2.1
Individual	619	33 \pm 1	3.89 \pm 0.65	30.4 \pm 0.9
Group	1042	32 \pm 1	3.62 \pm 0.51	31.1 \pm 1.3
Full	1799	32 \pm 1	3.33 \pm 0.49	31.2 \pm 1.3

Table 8: Context overhead analysis comparing minimal vs. full configurations. The 7.6x context increase results in faster inference (-19.7% total time) and negligible memory overhead (+0.7%), demonstrating efficiency of context-rich prompting.

Metric	Minimal	Full	Change	Relative
Context Size	237 chars	1799 chars	+1562	+659%
TTFT	33ms	32ms	-1ms	-3.6%
Total Time	4.15s	3.33s	-0.82s	-19.7%
Throughput	30.2 tok/s	31.2 tok/s	+1.0	+3.3%
Memory	5.02GB	5.05GB	+0.04GB	+0.7%

Future work should explore constrained decoding approaches that enforce structural consistency, hybrid architectures combining LLM reasoning with statistical error buffering, or training objectives that explicitly optimize for robustness under context drift.

4.3 Analysis and Insights

4.3.1 Modality-Specific Context Dependencies. To understand when context engineering provides value versus when it introduces unnecessary complexity, we conducted systematic ablation comparing minimal, individual, group, and full context across modalities. Results reveal modality-specific dependencies:

Table 9: Simulation Mode Performance. All LLM approaches exhibit severe degradation due to cascading error propagation, with conversation similarity collapsing by 83-99% relative to intervention mode.

Method	Conv Sim	Prox Sim	Degradation
Few-Shot (Similar)	0.007	0.425	-99.1%
SFT	0.165	0.104	-82.8%
Stratified Random	0.993	0.145	–

- **Conversation: Ceiling Effect.** Conversation achieves 97-100% weighted Jaccard *regardless of context level*, demonstrating that conversation patterns in constant-interaction collaborative tasks are highly predictable from persistence alone. Additional context provides no measurable benefit (paired t-test: $t=-1.89$, $p=0.065$, not significant).
- **Proximity: Context-Dependent.** Proximity improves from 0% (minimal context) to 6% (full context), a statistically significant gain (paired t-test: $t=3.42$, $p=0.001$, Cohen’s $d=0.63$, medium-large effect size). This indicates spatial coordination benefits from behavioral and structural context.
- **Shared Attention: Missing Features.** Shared attention remains at 0% across all conditions, indicating missing visual features (gaze target semantics) rather than insufficient context engineering.
- **Implications for Sensor Allocation.** These findings motivate a tiered sensing strategy: (1) audio-only sensing suffices for conversation (>95% accuracy), (2) audio + position tracking enables proximity prediction with context, and (3) gaze tracking with semantic object recognition is required for shared attention. This guides efficient resource allocation in future collaborative sensing deployments.

Table 10: Few-Shot Strategy Comparison ($k = 1$). Sociogram similarity in intervention mode across example selection strategies. Computational complexity indicates selection overhead (N = training set size).

Strategy	Sociogram Sim.	Selection Time
Random	0.579	$O(1)$
Phase Similar	0.582	$O(N \log N)$
Diverse	0.554	$O(N^2)$

4.3.2 Few-Shot Example Selection Strategies. Due to Gemma-2B’s 8K context window and substantial per-example token costs (approximately 4,552 tokens for full context and predictions), we evaluated three single-example selection strategies ($k=1$): random sampling, phase-similar selection (cosine similarity in MURMR’s 128-dimensional temporal phase embeddings [42]), and diversity-based selection (k -means++ initialization). The results are summarize in Table 10.

Phase-similar selection achieves marginally better performance (0.582 vs 0.579), representing only 0.5% relative improvement. The minimal performance difference suggests that Gemma-2B extracts relevant reasoning patterns from any contextually appropriate example, rather than requiring precisely matched demonstrations. Given the negligible benefit and substantial computational overhead ($O(N \log N)$ vs $O(1)$), random selection presents a compelling cost-benefit tradeoff for deployment scenarios.

4.3.3 Supervised Fine-Tuning: Configuration Insights. We adapted Gemma-2B using LoRA (rank $r = 16$, scaling factor $\alpha = 32$) targeting query, value, and output projection matrices, yielding approximately 2.5 million trainable parameters (0.10% of base model). Training used AdamW optimizer with learning rate 10^{-4} , effective batch size 8, and 3 epochs on Groups 1-12 (402 examples), achieving 99.04% token-level accuracy on held-out validation examples.

Critical Configuration: Sequence Length. Initial training attempts using Gemma-2B’s default tokenizer maximum length (1,024 tokens) resulted in severe truncation issues. Our full training examples require approximately 4,552 tokens (1,299 tokens for input context, 3,253 tokens for complete 6-pair predictions). Truncation at 1,024 tokens prevented the model from observing complete output targets during training, causing it to learn incomplete generation patterns (stopping after 1-2 pairs instead of 6). We resolved this by explicitly setting `tokenizer.model_max_length = 8192`, accommodating full examples with safety margin. Validation experiments confirmed the fix: truncated models generated only 2/6 complete pairs (33%), while corrected models produced all 6/6 pairs (100%), representing a 164.6% improvement in output completeness.

Loss Masking. We apply causal attention masking to compute cross-entropy loss exclusively on generated prediction tokens, excluding input context tokens. This design choice is critical: without masking, the model could reduce loss by simply learning to reconstruct input patterns (28.5% of the sequence), rather than learning the context-to-prediction mapping. Loss masking forces the model to attend to task-relevant features for behavior forecasting.

5 Discussion

Our evaluation reveals fundamental differences between statistical and semantic approaches to group behavior prediction, with implications for collaborative sensing systems and theoretical validation.

5.1 The Semantic Reasoning Gap

The context plateau, where LSTMs achieve 29% performance regardless of context richness, demonstrates an architectural limitation. Statistical models process behavioral clusters, network metrics, and temporal phases as numerical features without understanding their *meaning*. Predicting coordination requires compositional reasoning about how social roles interact with group states, not just pattern matching [22]. For our group coordination task, this suggests that richer context benefits prediction only when models can interpret the semantic relationships between behavioral patterns, structural properties, and temporal dynamics.

5.2 LLM Success and Constraints

LLMs achieve $3.2\times$ improvement (96% vs 30% for conversation) but exhibit critical limitations. **Modality-dependent performance** stems from task characteristics: conversation follows predictable turn-taking patterns LLMs capture effectively, while shared attention fails (0% recall) due to extreme class imbalance (1:200), missing visual semantics, and discrete tokenization poorly representing geometric gaze alignment. **Simulation brittleness** (83-99% degradation) arises from cascading context corruption where mispredicted edges corrupt density/reciprocity metrics, biasing subsequent predictions. Immediate collapse (half-life ≤ 2 windows) suggests constrained decoding, hybrid architectures with statistical error buffering, or periodic ground truth injection could extend prediction horizons. **Few-shot efficiency** reveals random selection performs comparably to sophisticated retrieval (0.5% difference), supporting cost-effective deployment.

5.3 System Design Implications

Results motivate a **tiered sensing strategy** based on what each modality requires: audio-only suffices for conversation ($>95\%$ from temporal patterns alone, context adds no benefit), audio + position tracking needed for proximity (spatial data essential, with 6% additional gain from behavioral/structural context), eye-tracking + semantic object recognition required for attention (currently fails at 0% due to missing visual semantics). **Deployment paradigms** differ where intervention mode (96%, sub-35ms latency) suits real-time coordination support, while simulation mode requires improvements but enables scenario planning where qualitative trends matter more than precise predictions.

5.4 Theoretical Validation and Limitations

The 96% predictive accuracy validates the IPO model [15] which indicates team processes exhibit systematic patterns driven by interpretable context, not stochastic dynamics. The context plateau empirically supports Social Identity Theory’s claim that coordination requires *semantic interpretation* of contextual cues [45]. However, our evaluation uses a single collaborative task with 4-person groups in MR settings, limiting generalizability to tasks with intermittent communication, larger teams, and physical collaboration. Future

work should explore vision-language models with coordinate embeddings for spatial reasoning [6], hybrid architectures combining LLM semantic reasoning with statistical error buffering for robust autoregressive prediction, and evaluation beyond structural metrics to measure intervention effectiveness and simulation fidelity in real deployments.

6 Conclusion

In this work, we demonstrated how LLMs can leverage hierarchical contextual information to predict group coordination patterns in collaborative MR environments, achieving $3.2\times$ improvement over statistical baselines through semantic reasoning about behavioral roles, network structure, and temporal dynamics. By transforming multimodal sensor streams into natural language, **M-CALLM** enables real-time coordination support with sub-35ms latency while revealing fundamental limitations: statistical models plateau regardless of context richness, and simulation mode brittleness exposes cascading error vulnerabilities. Looking ahead, we believe the success of future collaborative sensing systems will depend on their ability to balance semantic reasoning with specialized modules for spatial prediction, adaptively allocate sensing resources across interaction modalities, and navigate privacy-utility tradeoffs—as MR collaboration becomes ubiquitous, the next generation of group sensing will be defined by how effectively it weaves together real-time sensor observations, hierarchical behavioral context, and adaptive language model reasoning to deliver meaningful interventions that respect both architectural constraints and ethical boundaries.

Acknowledgments

This work is supported by the U.S. National Science Foundation (NSF) under grant number 2339266.

References

- [1] Mohsin Y Ahmed, Sean Kenkeremath, and John Stankovic. 2015. Socialsense: A collaborative mobile platform for speaker and mood identification. In *European Conference on Wireless Sensor Networks*. Springer, 68–83.
- [2] Kittipat Apicharttrisorn, Xukan Ran, Jiasi Chen, Srikanth V Krishnamurthy, and Amit K Roy-Chowdhury. 2019. Frugal following: Power thrifty object detection and tracking for mobile augmented reality. In *Proceedings of the 17th conference on embedded networked sensor systems*. 96–109.
- [3] Sizhen Bian, Vitor F Rey, Junaid Younas, and Paul Lukowicz. 2019. Wrist-worn capacitive sensor for activity and physical collaboration recognition. In *2019 IEEE International Conference on Pervasive Computing and Communications Workshops (PerCom Workshops)*. IEEE, 261–266.
- [4] Tom Brown, Benjamin Mann, Nick Ryder, Melanie Subbiah, Jared D Kaplan, Prafulla Dhariwal, et al. 2020. Language models are few-shot learners. *Advances in neural information processing systems* 33 (2020), 1877–1901.
- [5] Eugene Chai, Kittipat Apicharttrisorn, Limin Wang, Hyunseok Chang, and Sarit Mukherjee. 2025. PointPresence: An Online Habitat for Multi-User Mixed Reality Telepresence. In *Proceedings of the 23rd Annual International Conference on Mobile Systems, Applications and Services*. 277–290.
- [6] Xi Chen, Xiao Wang, Soravit Changpinyo, Anthony J Piergiovanni, Piotr Padlewski, Daniel Salz, Sebastian Goodman, Adam Grycner, Basil Mustafa, Lucas Beyer, et al. 2022. Pali: A jointly-scaled multilingual language-image model. *arXiv preprint arXiv:2209.06794* (2022).
- [7] Jonathon N Cummings and Rob Cross. 2003. Structural properties of work groups and their consequences for performance. *Social networks* 25, 3 (2003), 197–210.
- [8] Anind K Dey. 2001. Understanding and using context. *Personal and ubiquitous computing* 5, 1 (2001), 4–7.
- [9] Anind K Dey, Gregory D Abowd, and Daniel Salber. 2001. A conceptual framework and a toolkit for supporting the rapid prototyping of context-aware applications. *Human-computer interaction* 16, 2-4 (2001), 97–166.
- [10] Nathan Eagle and Alex Pentland. 2006. Reality mining: sensing complex social systems. *Personal and ubiquitous computing* 10, 4 (2006), 255–268.
- [11] Salma Elmalaki, Lucas Wanner, and Mani Srivastava. 2015. Caredroid: Adaptation framework for android context-aware applications. In *Proceedings of the 21st Annual International Conference on Mobile Computing and Networking*. 386–399.
- [12] Sepp Hochreiter and Jürgen Schmidhuber. 1997. Long short-term memory. *Neural computation* 9, 8 (1997), 1735–1780.
- [13] Edward J Hu, Yelong Shen, Phillip Wallis, Zeyuan Allen-Zhu, Yuanzhi Li, Shean Wang, Lu Wang, and Weizhu Chen. 2021. LoRA: Low-rank adaptation of large language models. *arXiv preprint arXiv:2106.09685* (2021).
- [14] Edward J Hu, Yelong Shen, Phillip Wallis, Zeyuan Allen-Zhu, Yuanzhi Li, Shean Wang, Lu Wang, Weizhu Chen, et al. 2022. Lora: Low-rank adaptation of large language models. *ICLR* 1, 2 (2022), 3.
- [15] Daniel R Ilgen, John R Hollenbeck, Michael Johnson, and Dustin Jundt. 2005. Teams in organizations: From input-process-output models to IMOI models. *Annu. Rev. Psychol.* 56 (2005), 517–543.
- [16] Ming Jin, Shiyu Wang, Lintao Ma, Zhixuan Chu, James Y Zhang, Xiaoming Shi, Pin-Yu Chen, Yuxuan Liang, Yuan-Fang Li, Shirui Pan, et al. 2023. Time-lm: Time series forecasting by reprogramming large language models. *arXiv preprint arXiv:2310.01728* (2023).
- [17] Rhee M Kil, Seon Hee Park, and Seunghwan Kim. 1997. Optimum window size for time series prediction. In *Proceedings of the 19th Annual International Conference of the IEEE Engineering in Medicine and Biology Society 'Magnificent Milestones and Emerging Opportunities in Medical Engineering' (Cat. No. 97CH36136)*, Vol. 4. IEEE, 1421–1424.
- [18] J Taery Kim, Archit Naik, Isuru Jayarathne, Sehoon Ha, and Jouh Yeong Chew. 2024. Modeling social interaction dynamics using temporal graph networks. In *2024 33rd IEEE International Conference on Robot and Human Interactive Communication (ROMAN)*. IEEE, 2272–2278.
- [19] Taemie Kim, Erin McFee, Daniel Olgun, Ben Waber, and Alex “Sandy” Pentland. 2012. Sociometric badges: Using sensor technology to capture new forms of collaboration. *Journal of Organizational Behavior* 33, 3 (2012), 412–427.
- [20] Takeshi Kojima, Shixiang Shane Gu, Machel Reid, Yutaka Matsuo, and Yusuke Iwasawa. 2022. Large language models are zero-shot reasoners. *Advances in neural information processing systems* 35 (2022), 22199–22213.
- [21] Benedek Kurdi, Shayn Lozano, and Mahzarin R Banaji. 2017. Introducing the open affective standardized image set (OASIS). *Behavior research methods* 49, 2 (2017), 457–470.
- [22] Brenden Lake and Marco Baroni. 2018. Generalization without systematicity: On the compositional skills of sequence-to-sequence recurrent networks. In *International conference on machine learning*. PMLR, 2873–2882.
- [23] Nale Lehmann-Wissenbeck and Joseph A Allen. 2018. Modeling temporal interaction dynamics in organizational settings. *Journal of business and psychology* 33, 3 (2018), 325–344.
- [24] Stephen C Levinson. 2016. Turn-taking in human communication—origins and implications for language processing. *Trends in cognitive sciences* 20, 1 (2016), 6–14.
- [25] Hong Lu, AJ Bernheim Brush, Bodhi Priyantha, Amy K Karlson, and Jie Liu. 2011. Speakersense: Energy efficient unobtrusive speaker identification on mobile phones. In *International conference on pervasive computing*. Springer, 188–205.
- [26] Hong Lu, Wei Pan, Nicholas D Lane, Tanzeem Choudhury, and Andrew T Campbell. 2009. Soundsense: scalable sound sensing for people-centric applications on mobile phones. In *Proceedings of the 7th international conference on Mobile systems, applications, and services*. 165–178.
- [27] Hong Lu, Jun Yang, Zhigang Liu, Nicholas D Lane, Tanzeem Choudhury, and Andrew T Campbell. 2010. The jigsaw continuous sensing engine for mobile phone applications. In *Proceedings of the 8th ACM conference on embedded networked sensor systems*. 71–84.
- [28] Haojie Ma, Zhijie Zhang, Wenzhong Li, and Sanglu Lu. 2021. Unsupervised human activity representation learning with multi-task deep clustering. *Proceedings of the ACM on Interactive, Mobile, Wearable and Ubiquitous Technologies* 5, 1 (2021), 1–25.
- [29] John E Mathieu, Tonia S Heffner, Gerald F Goodwin, Eduardo Salas, and Janis A Cannon-Bowers. 2000. The influence of shared mental models on team process and performance. *Journal of applied psychology* 85, 2 (2000), 273.
- [30] Daniel A McFarland, James Moody, David Diehl, Jeffrey A Smith, and Reuben J Thomas. 2014. Network ecology and adolescent social structure. *American sociological review* 79, 6 (2014), 1088–1121.
- [31] Emiliano Miluzzo, Nicholas D Lane, Kristóf Fodor, Ronald Peterson, Hong Lu, Mirco Musolesi, Shane B Eisenman, Xiao Zheng, and Andrew T Campbell. 2008. Sensing meets mobile social networks: the design, implementation and evaluation of the cenceme application. In *Proceedings of the 6th ACM conference on Embedded network sensor systems*. 337–350.
- [32] Chris Moore, Philip J Dunham, and Phil Dunham. 2014. *Joint attention: Its origins and role in development*. Psychology Press.
- [33] Daniel Olgun Olgun and Alex Sandy Pentland. 2008. Social sensors for automatic data collection. *AMCIS 2008 Proceedings* (2008), 171.
- [34] Jorge Luis Reyes Ortiz. 2015. Smartphone-based human activity recognition. (2015).

[35] Joon Sung Park, Joseph O'Brien, Carrie Jun Cai, Meredith Ringel Morris, Percy Liang, and Michael S Bernstein. 2023. Generative agents: Interactive simulacra of human behavior. In *Proceedings of the 36th annual ACM symposium on user interface software and technology*. 1–22.

[36] Liangying Peng, Ling Chen, Zhenan Ye, and Yi Zhang. 2018. Aroma: A deep multi-task learning based simple and complex human activity recognition method using wearable sensors. *Proceedings of the ACM on Interactive, Mobile, Wearable and Ubiquitous Technologies* 2, 2 (2018), 1–16.

[37] Alex Pentland. 2010. *Honest signals: how they shape our world*. MIT press.

[38] Giorgio Piatti, Zhijing Jin, Max Kleiman-Weiner, Bernhard Schölkopf, Mrinmaya Sachan, and Rada Mihalcea. 2024. Cooperate or collapse: Emergence of sustainable cooperation in a society of llm agents. *Advances in Neural Information Processing Systems* 37 (2024), 111715–111759.

[39] Aditya Ramesh, Prafulla Dhariwal, Alex Nichol, Casey Chu, and Mark Chen. 2022. Hierarchical text-conditional image generation with clip latents. *arXiv preprint arXiv:2204.06125* 1, 2 (2022), 3.

[40] Zhiwei Ren, Junbo Li, Minjia Zhang, Di Wang, Xiaoran Fan, and Longfei Shangguan. 2025. Toward Sensor-In-the-Loop LLM Agent: Benchmarks and Implications. In *Proceedings of the 23rd ACM Conference on Embedded Networked Sensor Systems*. 254–267.

[41] Diana Romero, Yasra Chandio, Fatima Anwar, and Salma Elmalaki. 2025. MoCoMR: A Collaborative MR Simulator with Individual Behavior Modeling. In *Proceedings of the 3rd International Workshop on Human-Centered Sensing, Modeling, and Intelligent Systems*. 114–119.

[42] Diana Romero, Yasra Chandio, Fatima Anwar, and Salma Elmalaki. 2025. MURMR: A Multimodal Sensing Framework for Automated Group Behavior Analysis in Mixed Reality. *arXiv preprint arXiv:2507.11797* (2025).

[43] Clayton Shepard, Ahmad Rahmati, Chad Tossell, Lin Zhong, and Phillip Kortum. 2011. LiveLab: measuring wireless networks and smartphone users in the field. *ACM SIGMETRICS Performance Evaluation Review* 38, 3 (2011), 15–20.

[44] Xiaoming Shi, Siqiao Xue, Kangrui Wang, Fan Zhou, James Zhang, Jun Zhou, Chenhao Tan, and Hongyuan Mei. 2023. Language models can improve event prediction by few-shot abductive reasoning. *Advances in Neural Information Processing Systems* 36 (2023), 29532–29557.

[45] Henri Tajfel, John Turner, William G Austin, and Stephen Worchel. 2001. An integrative theory of intergroup conflict. *Intergroup relations: Essential readings* (2001), 94–109.

[46] Paola Tubaro, Louise Ryan, and Alessio D'angelo. 2016. The visual sociogram in qualitative and mixed-methods research. *Sociological Research Online* 21, 2 (2016), 180–197.

[47] Ashish Vaswani, Noam Shazeer, Niki Parmar, Jakob Uszkoreit, Llion Jones, Aidan N Gomez, Łukasz Kaiser, and Illia Polosukhin. 2017. Attention is all you need. *Advances in neural information processing systems* 30 (2017).

[48] Roel Vertegaal. 1999. The GAZE groupware system: mediating joint attention in multiparty communication and collaboration. In *Proceedings of the SIGCHI conference on Human Factors in Computing Systems*. 294–301.

[49] David A Wasserman, Anita L Stewart, and Kevin L Delucchi. 2001. Social support and abstinence from opiates and cocaine during opioid maintenance treatment. *Drug and alcohol dependence* 65, 1 (2001), 65–75.

[50] Jason Wei, Xuezhi Wang, Dale Schuurmans, Maarten Bosma, Fei Xia, Ed Chi, Quoc V Le, Denny Zhou, et al. 2022. Chain-of-thought prompting elicits reasoning in large language models. *Advances in neural information processing systems* 35 (2022), 24824–24837.

[51] Anita Williams Woolley, Christopher F Chabris, Alex Pentland, Nada Hashmi, and Thomas W Malone. 2010. Evidence for a collective intelligence factor in the performance of human groups. *science* 330, 6004 (2010), 686–688.

[52] Ying Yang, Tim Dwyer, Michael Wybrow, Benjamin Lee, Maxime Cordeil, Mark Billinghamurst, and Bruce H Thomas. 2022. Towards immersive collaborative sensemaking. *Proceedings of the ACM on Human-Computer Interaction* 6, ISS (2022), 722–746.

[53] Yanxia Zhang, Jeffrey Olenick, Chu-Hsiang Chang, Steve WJ Kozlowski, and Hayley Hung. 2018. TeamSense: assessing personal affect and group cohesion in small teams through dyadic interaction and behavior analysis with wearable sensors. *Proceedings of the ACM on Interactive, Mobile, Wearable and Ubiquitous Technologies* 2, 3 (2018), 1–22.

[54] Qinlin Zhao, Jindong Wang, Yixuan Zhang, Yiqiao Jin, Kajie Zhu, Hao Chen, and Xing Xie. 2023. Competeai: Understanding the competition dynamics in large language model-based agents. *arXiv preprint arXiv:2310.17512* (2023).

Received 20 February 2007; revised 12 March 2009; accepted 5 June 2009